Published in final edited form as:
Exp Brain Res. 2007 June ; 180(2): 247–262. doi:10.1007/s00221-007-0852-0.

Reading in a Deep Orthography: Neuromagnetic Evidence for Dual-Mechanisms

Tony W. Wilson[1], **Arthur C. Leuthold**[2,CA], **John E. Moran**[3], **Patricia J. Pardo**[2], **Scott M. Lewis**[2], and **Apostolos P. Georgopoulos**[2]

[1]Neuromagnetic Imaging Center, Department of Psychiatry, University of Colorado Health Sciences Center, Denver, CO

[2]Brain Sciences Center, Veterans Affairs Medical Center, Minneapolis, MN

[3]Department of Neurology, Henry Ford Hospital, Detroit, MI

Abstract

Despite substantial efforts to connect cognitive-linguistic models with appropriate anatomical correlates, the question of which cognitive model best accounts for the neuropsychological and functional neuroimaging evidence remains open. The two most popular models are grounded in conceptually different bases and thus make quasi-distinct predictions in regard to the patterns of activation that should be observed in imaging investigations of linguistic processing. Dual-mechanism models propose that high-frequency regular and irregular words are processed through a lexicon-based word code, which facilitates their processing and pronunciation latencies relative to pseudowords. In contrast, single-mechanism models suggest the same behavioral effects can be explained through semantic mediation without the existence of a lexicon. In most previous studies, words and pronounceable pseudowords were presented in lexical-decision or word reading paradigms, and hemodynamic techniques were utilized to distinguish involved anatomical areas. The results typically indicated that both word classes activated largely congruent tissues, with a magnitude advantage for pseudowords in most or all activated regions. However, since the dual-mechanism model predicts both word types utilize the entire linguistic network, but that certain operations are merely obligatorily involved, these results do not sharply refute nor clearly support the model's main tenets. In the current study, we approach the dual- versus single mechanism question differently by focusing on the temporal dynamics of MEG imaged neuronal activity, during performance of an oddball version of continuous lexical-decision, to determine whether the onset latency of any cortical language region shows effects of word class that are indicative of preferential versus obligatory processing pathways. The most remarkable aspect of our results indicated that both words and pseudowords initially activate the left posterior fusiform region, but that the spatiotemporal dynamics clearly distinguish the two word classes thereafter. For words, this left fusiform activation was followed by engagement of the left posterior inferior temporal, and subsequently activation reached the left posterior superior temporal region. For pseudowords, this sequential order of left temporal area activations was reversed, as activity proceeded from the left fusiform to the left superior temporal and then the left inferior temporal region. For both classes, this dynamic sequential spread manifested within the first 300 ms of stimulus processing. We contend these results provide strong support for the existence of dual-mechanisms underlying reading in a deep orthographic language (i.e., English).

Mailing Address: Arthur C. Leuthold, Ph.D., Brain Sciences Center (4S), Veterans Affairs Medical Center (11B), One Veterans Drive, Minneapolis, MN 55417, Office: (612) 467-5546, Fax: (612) 725-2291, Email: E-mail: leuth004@umn.edu.

Keywords

word; MEG; temporal; fusiform; language

Introduction

This paper focuses on the neural implementation of reading in a quasi-regular or deep orthographic language, namely English. Reading in deep orthographies is complicated by mappings between graphemes, phonemes, and whole word sounds being inherently ambiguous. By comparison, languages with regular orthographies (e.g., German, Italian) are more transparent, as mappings between graphemes and phonemes are virtually one-to-one. Such straightforward grapheme-to-phoneme correspondence rules allow young readers to more rapidly acquire proficiency in reading (Frith et al. 1998; Landerl et al. 1997), and are associated with other benefits, like reduced pronunciation latencies, that extend well into adulthood (Paulesu et al. 2000).

Two different classes of cognitive models successfully account for the observed phenomena of reading complex orthography. These models are largely based on the behavioral and neuropsychological evidence that has accumulated over the last several decades. Both classes of models recognize at least two distinct reading strategies are necessary, as skilled English readers are able to pronounce words with regular spelling-to-sound relationships (e.g., kernel), as well as those with irregular relationships (e.g., colonel). However, the two classes differ in how these strategies are implemented in the model. Briefly, dual-mechanism models (Coltheart et al. 1993, 2001; Coltheart and Rastle 1994) assume orthography-to-phonology transformation can be achieved through two distinct mechanisms; the first is a lexical or whole-word procedure and the second a sublexical or assembled procedure. The postulated lexical method operates in parallel across the entire input string and would be engaged during processing of high-frequency words, especially those with irregular print-to-sound relationships. In contrast, the sublexical method is thought to operate serially from left-to-right, more or less assembling the word's phonological representation in piecemeal fashion. The sublexical procedure is necessary for novel or low-frequency words, as well as pronounceable pseudowords. Although, in the most recent formulation of this model, all words (e.g., high/low frequency, regular, and irregular) are processed in parallel through both mechanisms (Coltheart et al. 1993, 2001). The primary alternative to dual-mechanism accounts is a triangle-type interactive connectionist model (Plaut et al. 1996; Seidenberg and McClelland 1989). In this single-mechanism formulation, groups of simple units code orthographic, phonological, or semantic elements of the relevant corpus, and a word's pronunciation and meaning are represented as distributed patterns of activation across all units. Thus, words sharing phonological and/or semantic features would be represented by similar patterns of activation across the array of simple units, with particular print-to-sound correspondences being resolved through competitive and cooperative interactive processing amongst units in the network. Essentially, the triangle model includes one direct mechanism or route for orthography-phonology conversion, and a second indirect pathway implemented through semantics (Plaut et al. 1996). In addition, analogous to the dual-mechanism position, the single-mechanism account also postulates that all words are processed in parallel through both procedures, with irregular words being more reliant than regular on semantic mediation for successful processing. In short, these single- and dual-mechanism formulations share many common features, the primary distinction being whether the facilitation of word pronunciation is achieved through a semantic code (triangle-model) or a lexicon-based word code (dual-route model; for further discussion of these issues, see Binder et al. 2005).

Evidence for the neurological validity of these models arises from the neuropsychological literature, in particular lesion-based studies of acquired dyslexia. Most importantly, the existence of both phonological and surface dyslexia is congruent with distinct neural mechanisms subserving different processes for pseudo- and irregular word reading. In surface dyslexia, patients are able to read pronounceable pseudowords and unable to read irregular words, which suggests neural areas underlying lexical or semantic reading procedures have been selectively damaged. Conversely, patients with phonological dyslexia are able to read most high-frequency words (i.e., regular and irregular), but unable to process even simple pseudowords. Thus, in contrast to surface dyslexics, patients with phonological dyslexia seem to have selectively damaged neural areas serving sublexical conversion mechanisms. Overall, the existence of both disorders indicates at least partially distinct neural regions underlie the strategies for successful reading in deep orthographic languages. This idea of distinct neural systems tends to support models postulating partially discrete mechanisms for regular versus irregular words, and hence is congruent with both the dual-route and triangle-type formulations.

Another means of establishing such neurological validity is through the use of functional neuroimaging techniques in healthy readers. A benefit of using healthy volunteers to demarcate neural areas dedicated to reading is that it circumvents concerns of compensatory strategy use, as well as neural reorganization following neurological infarcts. On the other hand, these techniques only illuminate the neural tissues active, but not necessarily critical for any given cognitive process. Thus, it is possible that nodes recognized via functional neuroimaging are not absolutely necessary for successful performance. Word reading was one of the first cognitive feats to be investigated with functional neuroimaging (Petersen et al. 1988), and more than 15 years later this area remains one of the most active in cognitive neuroscience research. Yet, despite large amounts of empirical data, the neural mechanisms underling word and non-word reading remain an area of contention, especially for languages with deep orthographies. Many early studies used the seemingly straightforward word-pseudoword reading contrast, and reported largely non-replicable findings in regards to neural areas more active during word processing (for reviews, see Binder et al. 2003; Mechelli et al. 2003). This inconsistency may be reflective of the sufficient versus necessary confound acknowledged above; in short, the inability to reliably segregate neuronal activity in critical substrates from that in neural regions inessential to task performance (e.g., activation reflecting sublexical procedures during irregular word processing). Mechelli et al. (2002, 2003) have provided substantial evidence for this position by showing the same cortical areas are active during word and pseudoword processing, and that the major inconsistencies emerge when differences in activation magnitude are sought (i.e., when word- and pseudoword-induced activations are subtracted). Given this, the inconsistent findings reported in early studies of word versus pseudoword processing may have been attributable to very subtle differences in experimental design (e.g., stimuli, presentation parameters, etc.), functional organization (i.e., heterogeneity across subjects), and/or relatively small sample sizes (see Mechelli et al. 2003, for further discussion).

Regardless, more recent investigations of single and dual-mechanism models have been much more reliable, as numerous reading studies have found greater activation for pseudowords in both left occipitotemporal and inferior frontal regions (Binder et al. 2005a; Kronbichler et al. 2004; Mechelli et al. 2003; Paulesu et al. 2000; Xu et al. 2001). In addition, several studies using the lexical-decision task have reported greater activation for words in left occipitotemporal cortices, along with stronger or equivalent activation to pseudowords in left inferior frontal regions (Binder et al. 2003, 2005b; Fiebach et al. 2002; Ischebeck et al. 2004; Rissman et al. 2003). This pattern of results highlights the important issue of task-specific effects on neural areas more active during word or pseudoword processing. Essentially, multiple studies have collectively shown that only certain neural areas (e.g., left occipitotemporal) display strong task-specific responses to words and/or pseudowords, which potentially could provide useful information for discerning their particular role(s) in language

processing. Binder et al. (2003) noted that brain regions more active for words in the lexical-decision task closely match those normally detected in tasks probing semantic processing, which they interpreted as evidence supporting the single-mechanism triangle model of word processing (Plaut et al. 1996). Furthermore, by manipulating orthographic neighborhood density of words and pseudowords in the context of lexical decision, they demonstrated lexical candidates with high-density did not activate any brain area more than candidates with low neighborhood density (Binder et al. 2003). This latter result strongly suggests task performance is enabled by semantic units and not word-level units, as lexical candidates with high neighborhood densities should have elicited more activation than those with low-densities if performance were mediated by a non-semantic word-like code (i.e., a lexicon, as currently formulated in dual-route models; Coltheart et al. 1993, 2001). However, the existence of a lexicon-like neural word-form system remains a contentious matter, as other studies have shown word-frequency effects in regions corresponding to or near left occipitotemporal areas, which suggests word-level codes may indeed be involved in word reading (Keller et al. 2001; Kuo et al. 2003). In fact, Kronbichler et al. (2004) employed a sensitive parametric variation of word-frequency, and found strongly indicative evidence of a non-semantic word-like code mediating visual word recognition in left occipitotemporal cortex.

In our previous investigations, we reported that left perisylvian regions exhibit significantly earlier activation for words relative to pseudowords (Wilson et al. 2005a). This magnetoencephalography (MEG) study used the single-moving-dipole model for source localization, which is a good method for determining the location of compact sources. Of importance, a limitation associated with the single-dipole method involves its preference for focal versus highly-distributed sources. Basically, the method shows greater spatial precision, as well as fewer false negatives (i.e., failures to capture all ‘real’ sources) when the underlying activations are more focal in nature (Jerbi et al. 2004). This is a concerning factor in word/pseudoword comparisons, as intuitively one might expect pseudowords to elicit more diffuse activation in left-hemispheric cortices. Presumably, pseudowords induce a search process in which the linguistic system attempts to match the input to a possible lexical candidate, and such processing could elicit more distributed activation within neural regions mediating lexicality. Thus, it could be argued that pseudoword-induced sources are more commonly missed in single-dipole analyses. In the present work, we use a cortically-constrained distributed-source imaging technique to provide continuous and precise time courses for focal and diffuse neural activations, which is a substantial enhancement to our previous single-dipole investigations (e.g., Wilson et al. 2005a, Wilson et al. 2005b). After imaging cortical activity with this technique, we calculate the time series of local current-density amplitude within the regions-of-interest (ROI) most often acknowledged as critical to language processing. Extensive prior neuroimaging work has shown a small group of left hemispheric neural regions are reliably involved in word and pseudoword processing (for reviews, see Jobard et al. 2003; Mechelli et al. 2002, 2003; Price 2000; Price et al. 2003), and in the current analyses we chose to focus uniquely on these eloquent language cortices.

We hypothesized that differences in the time course of activated neural regions would distinguish the processing of words and pronounceable pseudowords. In other words, both types of lexical candidates will likely activate each region of interest (i.e., due to obligatory processes), but the relative timing of these activations should differ between the two classes of stimuli beyond what could be attributed to word-frequency effects. Essentially, if participants utilize a lexicon-like word-based code in processing real words, than preferential processing (i.e., shorter latencies) along this pathway should be discerned for words relative to pseudowords during the lexical-decision task. We believe detecting such temporal differences would provide strong evidence for the existence of dual-mechanisms or pathways for word processing (Coltheart et al. 1993, 2001), and that a lack of such differences would more support triangle-type formulations of word processing (Platt et al. 1996). To investigate

this, we conducted a MEG imaging study of regional brain activation during an oddball version of the lexical-decision paradigm. Our primary aim was to quantify temporal activation differences, between high-frequency words and pronounceable pseudowords, in each of the most recognized cortical regions subserving language processing. To illuminate the cortical dynamics, we also transformed spatiotemporal current-density estimations into statistical parametric maps (dSPM) reflecting region-specific time courses of neuronal activation.

Materials and Methods

Participants

Eleven native English speakers age 18–41 years (mean: 28 years) were paid to participate in this experiment (8 males and 3 females). One male subject's data was discarded due to excessive blinking. All subjects were strongly right-handed as assessed by the Edinburgh Handedness Inventory (range: 75–100; Oldfield 1971). All subjects had normal or corrected to normal vision, and denied any history of neurological or psychiatric disease (including drug/alcohol abuse). Each subject provided informed consent to a protocol approved by the Institutional Review Boards of the University of Minnesota and the Veterans Affairs Medical Center, Minneapolis, Minnesota.

Experimental Paradigm

Subjects performed an oddball version of the lexical-decision task while supine in a dimly lit, magnetically shielded room (MSR). The stimulus set included 120 concrete nouns, 100 pronounceable pseudowords, and 80 consonant strings. From these stimuli, 40 concrete nouns and 20 pseudowords were randomly selected to serve as targets. The two-syllable concrete nouns were of high-frequency (range: 1.12 – 1.84 log; mean: 1.49 log; Kucera and Francis 1967), and all followed regular orthography-to-phonology conversion principles (i.e., irregular or exception words were not permitted). To create pseudowords, we shuffled the phonemes of the concrete nouns; thus, phonemic units present in the corpus of words were preserved in the pseudowords, and the two types of stimuli did not significantly differ in mean positional bigram frequency (mean(SD); words: 1722.6(867.9), pseudowords: 1635.5(809.4)), neighborhood density (words: 5.4(4.4), pseudowords: 5.1(3.3)), or total number of characters (words: 4.5 (0.6), pseudowords: 4.5(0.6); Balota et al. 2002). Particular care was also taken to ensure pseudowords resembled real English words in all respects, with the exception of lexical and semantic status (i.e., we screened for pseudohomophones and other 'special' pseudowords). We included consonant strings only for comparison to earlier experiments, thus these data will be reported separately. The experiment consisted of 6 blocks, each lasting approximately 60 seconds with a 15-second inter-block interval. Thus, overall recording time was ~8 minutes. In each block, participants viewed (duration = 600 ms; stimulus-onset-asynchrony = 1200 ms) 40 non-targets and 10 targets in a pseudo-randomized order. The 10 targets were all words in four blocks and all pseudowords in the remaining blocks. In blocks where words served as targets, participants saw, on average, the same number of non-target pseudowords and consonant strings within each block. In the other two blocks, participants saw only the 10 pseudoword targets and the 40 non-target real words (i.e., no consonant strings). For each participant, the sequential order of blocks was re-randomized, as was the order of stimuli within each block. All stimuli were 4–6 letters long and presented only once in white 36-point Courier font on a black background. Stimulus presentation alternated with a white fixation cross. Subjects responded with a button press when a target was observed, and did not respond to other stimuli (i.e., go/no-go task). Before MEG acquisition, subjects were asked to limit blinking during stimulus presentation. However, during the inter-block intervals, subjects were told via visual display to blink freely, and were also notified of which word-type would function as the target stimuli in the ensuing block. All stimuli were presented using the STIM software

(Compumedics Neuroscan, El Paso, TX). An LCD projector outside the MSR projected all stimuli and instructional messages onto a screen positioned ~60 cm above the subject.

MEG Acquisition and Data Processing Procedures

With an acquisition bandwidth of 0.1–200 Hz, neuromagnetic signals were sampled continuously at 508 Hz using a Magnes 3600 WH equipped with 248 axial-gradiometers (4-D Neuroimaging Inc., San Diego, CA). Each axial-gradiometer is coupled to a SQUID sensor, which acts as a low-noise magnetic flux-to-voltage converter. Along with the magnetic data, a photodiode signal (to ensure precise timing in stimulus delivery) and an electrooculogram (EOG) were also recorded. The continuous MEG data stream was exported from the acquisition environment, and cardio-corrected in its continuous native format. All cardiac artifacts were removed from each subject's MEG data series using the event-synchronous subtraction method (Leuthold 2003). This method of cardio-artifact removal uses a computer algorithm, along with user input, to identify each QRS complex of the cardiac artifact waveform infiltrating the most susceptible MEG sensors. Each P through T heartbeat is then averaged within each sensor individually throughout the acquisition period. In turn, this averaged heartbeat artifact, particular to a given sensor, is subtracted from each heartbeat within the respective sensor's time series. Next, all MEG data were digitally filtered using a 30 Hz low-pass butterworth filter and split into 1 s epochs (including a 200 ms pre-stimulus baseline), with zero defined as the time-point of stimulus onset. We used a fixed threshold method (EOG > 100 uV or MEG level > 1.25 pT), supplemented with visual inspection, to identify and reject artifactual epochs. Furthermore, epochs in which the subject behaviorally responded were also rejected (i.e., correct button presses to targets and incorrect to non-targets). For each word type, at least 60 trials (out of 80 possible) remained and an average response was calculated for each. Average responses were baseline corrected by subtracting the signal amplitude of the 200 ms pre-stimulus time interval. With the exception of cardio-correction, MEG data were preprocessed using Brain Electrical Source Analysis Software (BESA, Version 5.0.4; MEGIS, Germany).

MRI Acquisition and Coregistration with MEG

Anatomic images of the brain were acquired on a General Electric Signa Horizons LX 1.5T MR scanner using a neuro-vascular head coil. Sagittal scout images were taken to determine the number and placement of subsequent axial slices. The volume covered extended from the top of the head to the bottom of the cerebellum, including the external auditory meati bilaterally (thus, all MEG fiducial points were within coverage). T1-weighted axial images were then acquired using a 3-dimensional SPGR sequence with the following parameters: TE = minfull, TR = 20 ms, Flip angle = 30 deg., FOV = 240 × 240 mm, matrix = 256×256, slice thickness/gap = 1.5/0, NEX = 1. The resulting voxel resolution was 0.94 × 0.94 × 1.5 mm.

Prior to MEG measurement, five small coils were attached to the participant's head and the locations of these coils, together with the three fiducial points and scalp surface, were determined with a 3-D digitizer (Fastrak 3SF0002, Polhemus Navigator Sciences, Colchester, VT). Once the participant was positioned inside the helmet of the neuromagnetometer, a small electric current was fed to the coils, inducing a measurable magnetic field. This allowed the coils to be located in reference to the sensors. Since coil locations were also known in head coordinates, all MEG data could be transformed into a common coordinate system. Moreover, since the head coordinate system could be mapped onto the participant's MRI, individual MEG responses could also be mapped onto the structural MRI. Coregistration of MEG and MRI data was performed with the MEG Tools Imaging and Visualization Software (Moran and Tepley, Oakland University – Henry Ford Hospital Neuromagnetism Laboratory, Detroit, MI) implemented in MATLAB (Version 7.0, R14; The MathWorks, Inc., Natick, MA).

MEG Current-Density Imaging Procedures

Construction of head model and solution space—In contrast to EEG imaging, the locations of electrical sources can be accurately calculated for MEG data using a simple spherical volume conductor model of the head (Hämäläinen and Sarvas 1989). However, accuracy can be enhanced through a multi-sphere approach, in which several overlapping spherical models are each fit to the local curvature of a different brain region (Leahy et al. 1998). In this study, we approximated the brain as an overlapping series of six miniature spherical models, each optimally fit to the local curvature of a distinct brain region as discerned through MRI. To additionally enhance localization accuracy, all possible sources were confined to areas occupied by cortical gray matter. This constraint on source locations was implemented by converting the subject's MRI slice sequence into a 3D volume, and segmenting the skin/scalp region, skull region, CSF boundary, gray matter region, and white matter region based on the MRI pixel amplitude differences and boundary gradients between tissue types. Once the brain had been fully segmented, the gray matter was subdivided into ~3000 patches of equal volume and a discrete X,Y, and Z oriented dipole source was positioned at the center of each cortical gray matter patch. Thus, the cortical model did not constrain the orientation of primary source currents.

Calculation of current-density images—Multi-Resolution FOCUSS (MR-FOCUSS; Bowyer et al. 2004; Moran et al. 2001, 2005) is a whole brain current-density imaging technique designed to avoid imaging the noise component of MEG data. An initial estimate of cortical activity is recursively refined until the estimated residual (residual = recorded MEG signals – forward calculated field of estimated source activity) is mostly uncorrelated with brain activity at any source location in the cortical model. During each recursive step of the imaging algorithm, sources are ranked according to their importance in improving the estimated solution. Subsequently, source rank is used to assign how each source contributes to a set of 24 multi-resolution source basis structures. Transformation of the source model to a multi-resolution wavelet source basis enables MR-FOCUSS to control the sequence of both focal and extended changes that are made to the initial estimate of the source structure amplitudes. Focal source imaging characteristics of MR-FOCUSS are fine-tuned by specifying the exponent of an exponential cumulative distribution template, which is used to construct the multi-resolution wavelet source basis. In this study, we used an exponent of 0.8 ($l_{0.8}$ norm for source solution amplitudes) because the most significant sources contributing to the MEG data were expected to be relatively small and compact. However, using this exponent does not exclude the imaging of more extended source structures provided the activity is of sufficient amplitude; rather, the tradeoff is that weak activity is simply not imaged.

Using MR-FOCUSS, the time series of whole-brain current-density images was constructed for each event-related field (ERF) from each participant. To enhance statistical robustness of imaged activity against initialization bias, a set of 20 MR-FOCUSS solutions were created and averaged with each solution utilizing different initial estimate of source activity. For each cortical location, the x, y, and z initialization amplitudes were set equal to the goodness-of-fit between the MEG data and the corresponding source forward model. Next, these source amplitudes were multiplied by a set of random numbers (mean of zero and standard deviation of 1) generated by the MATLAB function, randn. Adding variability to the set of initialization structures improves the visibility of lower amplitude sources in the final output images (Moran et al. 2001, 2005). Thus, the final average estimates of brain activity were only partly influenced by the local ECD-metric goodness-of-fit to the MEG data. The MR-FOCUSS current-density imaging protocol is part of the standard MEG Tools software package, and in the present study was implemented in MATLAB (Version 7.0, R14). Further details concerning the MR-FOCUSS technique are available (Moran et al. 2005).

Current-density image processing—The output of the MR-FOCUSS imaging technique provided source amplitudes for X, Y, and Z orientations of each source at ~3000 cortical locations across 1000 ms of neural activity contained in the original ERF. X, Y, and Z source amplitudes were summed in quadrature yielding a single time series (per condition, per subject) indexing the total current-density amplitude at each source location. This eliminated information on the orientation of the underlying currents, which was not required for our experimental goals.

Constructing Regions of Interest and Noise-Normalizing Amplitude Estimates

The paramount goal of this research involved elucidating the time course of core brain areas serving language processing. Thus, while it is highly probable these core brain areas are comprised of further specialized sub-regions, our analysis minimizes this effect and focuses on distinct brain regions as a whole. To that end, four ROIs including qualitatively the same neural structures were defined on each participant's MRI. These four left-hemispheric brain regions were chosen because extensive neuroimaging work has repeatedly identified them as the core network underlying language processing (for reviews, see Jobard et al. 2003; Mechelli et al. 2002, 2003; Price 2000; Price et al. 2003). The spatial extent of each ROI was defined in accordance with Duvernoy et al. (1999) and included the following neural structures in all participants: (1) the posterior third of the complete left fusiform gyrus (FUSIp), (2) the posterior third of the left inferior temporal sulcus, extending ventrally to include the corresponding gyrus in its entirety (ITG-Sp), (3) the posterior third of the left superior temporal gyrus and sulcus, extending dorsally to include the inferior aspects of the supramarginal gyrus (STG-Sp), and finally (4) the left inferior frontal gyrus from the anterior border of the pars orbitalis to the posterior border of the pars opercularis, including all of the pars triangularis (IFG).

The mean current-density amplitude per time slice was calculated by summing the amplitudes of all sources within each ROI, and dividing this number by the total number of sources comprising the ROI. Since each source represented an equal volume of gray matter, the mean ROI current-density amplitude was a preferable measure of brain activation as it could be reliably compared across ROIs that differed in absolute size. Thus, a single mean current-density amplitude time series was calculated for each ROI, which yielded four ROI-specific waveforms per subject and condition.

Once the mean current-density per time slice was known for each ROI, all activity estimates were noise-normalized by dividing the mean current-density per time slice by the predicted standard error of the estimate due to additive noise. This was done separately for each subject, by utilizing the ROI-specific baseline periods of the mean current-density calculations for both conditions. These noise-normalized estimates are approximately t-distributed under the null hypothesis of no cortical activity, and since a large number of data points are used to estimate the noise level inherent to each ROI, the t-distribution will generally approach a unit-normal distribution (i.e., a z-score; Dale et al. 2000). These noise-normalized activity estimates can be averaged across a sample and plotted to show the statistical reliability of cortical activity in each ROI as a function of time. Doing so offers an alternative vantage into the temporal dynamics of each cortical region, and also provides a medium for recognizing interesting time periods, which can then be further explored for effects related to the experimental manipulations. In this study, activation for a single time slice, in a given ROI, had to be at least 3 standard deviations above the noise level to be recognized as significant (i.e., z-score = 3; $p < 0.001$). Obviously, this is a somewhat arbitrary threshold, but the goal was not to say X region was more active than Y region. On the contrary, the goal was simply to recognize periods of significant signal, and investigate how these temporal windows differ as a function of word-type.

To further explore effects related to the experimental manipulations, difference waveforms were also constructed for each participant by subtracting the time series corresponding to the pseudoword condition from that of the word condition within each ROI. Following subtraction, the RMS (root-mean-square) amplitude differences across the 10 participants (per data point) were calculated and plotted for each ROI, which enabled identification of latency periods where the conditions seem to elicit reliably differential activation in a given ROI across our entire sample. Potential latency effects were then further investigated by using the original time course per subject and condition (i.e., the non-differenced data) in a series of ROI-specific repeated-measures analysis-of-variance (RM-ANOVA); to examine interaction effects, we used two-tailed, paired-samples t-tests. RM-ANOVA's account for the variation within a given sample and are virtually equivalent to the random-effects analyses more commonly used in fMRI. Basically, since these statistical procedures explicate the within-sample variance, they provide a venue for generalizing experimental results to the population. All statistical analyses used the Standard Version of SPSS for Windows (Release 11.0.1).

Results

Behavioral Data

Error rates for the lexical-decision task were too low for further analyses (mean: 2.53%). Subjects recognized real word stimuli faster than they rejected pseudoword stimuli (mean RT: words = 592 ms, pseudowords = 665 ms), and this difference was significant (paired t-test, $t(9) = 3.25$, $p < 0.01$). Thus, behavioral results attained through this oddball-variant of the lexical-decision task were consistent with typical observations, as words were accepted significantly faster than pseudowords were rejected.

Neural Data

The whole-brain MR-FOCUSS images indicated global activation patterns were only minimally affected by word-type, as activation for both words and pseudowords commenced in bilateral posterior occipital cortices ~80 ms after stimulus onset, and was typically sustained until ~135 ms in this brain region. Moreover, the spatial extent and time course of the initial anterior spread of activation did not indicate pronounced differences between the two conditions; although only potent effects would have been discernable from the whole-brain MR-FOCUSS images (i.e., brain activation movies). In addition to viewing as movies, we noise-normalized, averaged, and plotted current-density estimates to illuminate the temporal dynamics of significant activation during word and pseudoword processing (see Figure 1). As described in the Methods, the noise-normalized estimate for a single time slice, in a given ROI, had to be at least 3 standard deviations above the noise level to be recognized as significant (i.e., $p < 0.001$).

As shown in Figure 1, the time course of FUSIp cortices indicated words evoked an early oscillation peaking at ~61 ms post-stimulus onset. This activity was brief (duration: 18 ms) and had subsided by ~70 ms into the epoch. However, roughly ~25 ms later (onset: 98 ms; peak: 124 ms), a second oscillation of greater amplitude and duration (i.e., 65 ms) occurred in the FUSIp area, and this coincided with a burst of activity in the ITG-Sp (duration: 20 ms). By ~165 ms post-stimulus, activity in both regions had resolved and FUSIp cortices stayed below threshold for the remainder of word condition time series (see Figure 1). Words did not evoke significant activation again until 238 ms into the time course, when a significant fluctuation (duration: 43 ms; peak: 263 ms) in STG-Sp was detected. Following the offset of STG-Sp cortices, activation emerged at 352 ms in ITG-Sp and was shadowed by the first significant activity detected in the IFG (onset: 362 ms; duration: 39 ms). Activation dissipated in both regions shortly after 400 ms post-stimulus, but returned in parallel to these cortical areas at ~420 ms. For both regions, this second period of activation peaked at ~450 ms post-stimulus

(ITG-Sp peak: 450 ms; IFG peak: 448 ms); however, activity in ITG-Sp cortices remained significant for a much longer duration (ITG-Sp: 134 ms; IFG: 73 ms). Activity in IFG declined below significance after ~485 ms, and these cortices were idle for the remaining time course. In fact, only temporal regions showed activity persisting after ~500 ms. For the ITG-Sp, significant activity again emerged at 590 ms and was sustained until almost 730 ms. Meanwhile, activation culminated in the STG-Sp from 637–717 ms (Figure 1).

In contrast to words, pseudowords did not evoke the early ~60 ms oscillation in FUSIp cortices; instead, pseudoword-induced activation commenced with the larger second oscillation (onset: 92 ms), which followed a temporal envelope very similar to that observed in the word condition although with a much protracted duration (duration difference = 59 ms; see Figure 1). Within this same time window (i.e., 92–222 ms post-stimulus), two distinct oscillations were also elicited by pseudowords in STG-Sp. The first significant fluctuation in STG-Sp cortices peaked 112 ms, while the second emerged at 191 ms and peaked at 204 ms. The time course of all ROIs was devoid of significant activation from 220 ms until 260 ms, but shortly thereafter activity reemerged in the STG-Sp area (onset: 261 ms). This neural activation was followed by activity in FUSIp cortices (onset: 273 ms) and the IFG region (onset: 283 ms; peak: 297 ms). These ROI-specific fluctuations occurred in more-less temporal synchrony, or with short lags (Figure 1); thus, by ~275 ms into the time series, highly interactive processes may have been well underway. Activation in FUSIp and IFG rescinded below threshold after ~300 ms, but reemerged in both regions around ~330 ms, and the ITG-Sp time course indicated the initiation of processing shortly thereafter (i.e., ITG-Sp onset: 389 ms). Following the dissipation of FUSI-p activity, an extended period of activation ended in the STG-Sp (duration: 154 ms), which was followed by cessation of activity in IFG and finally ITG-Sp. For the remainder of the time series, IFG cortices reflected idle processing that never approached significance; however, a single oscillation was detected in both ITG-Sp (470–556 ms) and FUSIp (684–714 ms). Meanwhile, a series of four fluctuations culminated in STG-Sp cortices (464–554 ms, 584–657 ms, 670–731 ms, and 755–786 ms; see Figure 1).

While these average time courses provide substantial insight into the dynamics of language processing, they are governed by the pitfalls affecting all“mean” calculations. In short, extreme values in a subset of participants can tremendously determine the overall impression of a mean score. Thus, we further investigated these data to find spatiotemporal activation patterns that clearly coexisted in our group of participants. To achieve this, we constructed difference waveforms for each ROI and used these results to identify latency periods showing pronounced differences. These latency periods were then further tested using ROI-specific RM-ANOVAs on the original single-subject time courses. Below, we report the results attained through this procedure, starting with the most posterior brain region (i.e., FUSIp) and finishing with the IFG.

Regional Analyses

Conditional Dynamics of FUSIp Cortices—Difference waveforms revealed four potential latency bins of differential activation elicited during word or pseudoword processing; these periods were 40–75 ms, 185–355 ms, 535–585 ms, and 680–720 ms. After calculating within-subject means for these time periods, we performed a RM-ANOVA with condition (2 factors) and latency bin (4 factors) as within-subject variables, and the mean noise-normalized current-density estimate as the dependent measure.

The current data set violated the assumption of sphericity, so Huynh-Feldt Epsilon adjusted degrees of freedom were used to compute significance levels. The main effect of condition was significant $F(1,9) = 29.318$ ($p < 0.0001$), indicating more overall activation in the pseudoword condition. The effect of latency bin did not approach significance $F(1.9,16.8) = 0.967$ ($p > 0.35$), and the condition-by-latency bin interaction effect suggested only marginal

effects $F(1.3,11.9) = 2.39$ ($p = 0.144$). Nevertheless, we explored this interaction effect to discern whether greater activation to pseudowords was restricted to specific latency bins. As shown in Figure 2, paired-samples t-tests indicated significantly more pseudoword-elicited activation during the 185–355 ms latency bin $t(9) = -2.599$ ($p < 0.03$), and 680–720 ms latency period $t(9) = -3.185$ ($p < 0.01$). Significant effects were not detected for the other bins. Thus, FUSIp activation favored pseudowords overall, but only reliably discerned stimuli from 185–355 ms and 680–720 ms (Figure 2).

Conditional Dynamics of the ITG-Sp Region—Difference waveforms indicated five potential latency bins for differential activation between word classes; these time periods were 110–150 ms, 400–430 ms, 435–465 ms, 525–555ms, and 585–725 ms. To investigate, we again performed RM-ANOVA with condition and latency bin as within-subject variables, and mean noise-normalized current-density as dependent measure.

Mauchly's test of sphericity indicated the assumption of sphericity to be valid, thus all reported values assume sphericity. The effect of condition was not significant $F(1,9) = 2.567$ ($p > 0.14$), indicating overall activation in ITG-Sp cortices did not differ between word classes when collapsed across latency periods. However, the main effect of latency bin was significant $F(4,36) = 3.402$ ($p < 0.02$), and pairwise comparisons revealed greater activation during the 435–465 ms latency bin relative to 110–150 ms bin ($p < 0.025$) and that none of the other latency periods significantly differed from each other. The interaction effect was also significant $F(4,36) = 18.055$ ($p < 0.0001$), and within-subject contrasts indicated only the fourth order component was significant $F(1,9) = 46.403$ ($p < 0.0001$). Consistent with the previous analysis, we used two-tailed paired-samples t-tests to explore the interaction effect. As shown in Figure 3, this set of analyses indicated significantly more word-elicited activation from 110–150 ms $t(9) = 2.568$ ($p < 0.03$), and 435–465 ms $t(9) = 6.50$ ($p < 0.001$). Conversely, pseudoword stimuli evoked greater activation from 400–430 ms $t(9) = -4.676$ ($p < 0.002$), and 525–555 ms $t(9) = -2.832$ ($p < 0.025$). Lastly, the final latency bin did not show significant effects. In summary, ITG-Sp activation was more robust for words during the earliest (110–150 ms) and middle latency periods (435–465 ms) and stronger for pseudowords during the second (400–430 ms) and fourth (525–555 ms) latency bins (Figure 3).

Conditional Dynamics of STG-Sp Cortex—The difference waveforms approach yielded four time windows of interest, including 95–215 ms, 295–405 ms, 505–545 ms, and 585–645 ms. To explore this latency periods, we used a RM-ANOVA with condition (2 factors) and latency bin (4 factors) as within-subject variables, and mean noise-normalized current-density as dependent measure.

The assumption of sphericity held in these data, and all reported values assume sphericity. The main effect of condition was significant $F(1,9) = 9.356$ ($p < 0.015$), showing greater STG-Sp activation for pseudowords. The latency bin effect approached significance $F(3,27) = 2.804$ ($p < 0.06$), so we performed pairwise comparisons to illuminate more activation during the third (505–545 ms; $p < 0.05$) and fourth (585–645 ms; $p < 0.01$) latency windows relative to the earliest period (95–215 ms). The remaining pairwise comparisons did not show significant effects. The condition-by-latency bin interaction effect failed to reach significance $F(3,27) = 2.08$ ($p < 0.13$), but within-subject contrasts showed the linear component to be informative $F(1,9) = 6.805$ ($p < 0.03$). As shown in Figure 4, follow-up analyses (paired-samples t-tests) indicated significantly more robust activation to pseudoword stimuli during all latency bins (all p values < 0.05).

Conditional Dynamics of IFG Cortices—Difference waveforms indicated only three potential latency windows (i.e., 275–355 ms, 385–415 ms, and 425–485 ms) for differential activation between word classes. Consistent with prior regional analyses, we performed RM-

ANOVA with condition (2 factors) and latency bin (3 factors) as within-subject variables, and mean noise-normalized current-density as dependent measure.

Mauchly's test of sphericity indicated the assumption of sphericity held in these data, and all values reported here assume sphericity. The main effect of condition was not significant $F(1,9) = 4.314$ ($p > 0.065$), and neither was the latency bin effect $F(2,18) = 1.542$ ($p > 0.24$). However, the interaction effect was significant $F(2,18) = 20.507$ ($p < 0.0001$), and within-subject contrasts showed linear $F(1,9) = 27.13$ ($p < 0.002$) and quadratic components $F(1,9) = 13.626$ ($p < 0.005$) to be informative. As Figure 5 shows, pseudowords elicited reliably greater activity from 385–415 ms $t(9) = -2.408$ ($p < 0.04$), but the reverse effect of greater word-induced activity was observed in the 425–485 ms temporal period $t(9) = 4.364$ ($p < 0.002$). The earliest bin showed no reliable differences.

Discussion

The lexical-decision task has been used extensively in functional neuroimaging research on language processing, and in the present study we chose this same paradigm so that final analyses could be focused, with some degree of confidence, on only neural regions routinely identified as crucial to the cognitive processes. In doing so, we were able to perform an in-depth analysis of the neural dynamics underlying task performance, which in-turn provided a venue for deciphering whether a dual or single-mechanism model best accounted for activation patterns elicited by reading in a deep orthography.

First, when collapsed across time, significant activation was found in all four ROIs for both word classes in all subjects. This corresponds closely to research utilizing alternative imaging modalities such as fMRI and PET (Jobard et al. 2003; Mechelli et al. 2002, 2003; Price 2000; Price et al. 2003). Additionally, the cortical dynamics observed in our whole-brain MR-FOCUSS images were congruent with previous MEG language mapping studies that used similar methodological approaches (Dale et al. 2000; Dhond et al. 2001, Dhond et al. 2003; Marinkovic et al. 2003), as well as those employing spatial filtering and dipole modeling techniques (Cornelissen et al. 2003; Pammer et al. 2004; Simos et al. 2002). For example, our data corroborate past studies showing posterior fusiform cortices are active before 150 ms regardless of the stimuli's lexical status (Cornelissen et al. 2003; Dale et al. 2000; Marinkovic et al. 2003; Pammer et al. 2004; Simos et al. 2002). The earlier activation we detected to words in the left inferior temporal region has also been previously reported, as Pammer et al. (2004) detected an analogous effect by contrasting word and anagram stimuli during lexical-decision. However, this latency difference was not found in another study that compared the reading of exception words, pseudowords, and pseudohomophones (Simos et al. 2002), which may indicate the time course of left inferior temporal activation is task-dependent. Interestingly, the temporal behavior of left superior temporal activation may also be contingent on particular task requirements, as contrary to our results Simos et al. (2002) did not report a significant lexicality effect on activation latency in this neural region (i.e., earlier activation for pseudowords). Although in their study, a significant correlation was detected between the pronunciation latency of pseudowords and pseudohomophones, but not words, and the onset of activation in left superior temporal cortices (Simos et al. 2002), which suggests this area is critically involved in processing pseudowords and provides some credence to the idea that task variations may partially explain activation differences found across these studies. Overall, such MEG investigations have indicated substantial temporal complexity underlies the activation clusters commonly found through hemodynamic investigations. Below, we focus on the results of our regional analyses as they speak most directly to the impetus of the current experiment.

The neurological model of reading proposed by Price 2000) provides a clear framework for interpreting the spatiotemporal dynamics evoked by each condition, particularly in regard to

single- versus dual-mechanism accounts. In this model, processing of both words and pseudowords proceeds in parallel along two different paths. The left posterior fusiform gyrus serves as the origin for both pathways and potentially stores pre-lexical visual word-form information, such as the bigram regularities of a language (Cohen and Dehaene 2004; Dehaene et al. 2005). However, a related account has suggested these visual word-form representations are likely at the lexical-level (i.e., whole words), as word-frequency effects have been demonstrated in both left posterior and middle fusiform cortices (Kronbichler et al. 2004). Although at present, there are actually several alternative interpretations of left posterior fusiform function which have not been decisively refuted or accepted given, at least partially, the limited spatial resolution of current neuroimaging instrumentation. For example, Devlin et al. (2004) has showed sensitivity to orthographic but not semantic priming effects in this region, and argued the area is merely an orthographic processing center that likely serves as a perceptual interface for generating phonological representations from visual input (Devlin et al. 2006; Price and Devlin 2004; Price and Mechelli 2005). Nevertheless, for the current discussion, the important feature of Price's model is the proposal that posterior fusiform outputs code in parallel to both inferior and superior temporal gyri. Based on functional neuroimaging and neuropsychological evidence, the inferior temporal gyrus is considered a semantic area while superior temporal gyrus is recognized for phonological functions. Thus, posterior fusiform to inferior temporal gyrus connections are thought to constitute more of a semantic pathway, where words would receive preferential processing and perhaps top-down modulation from anterior IFG regions (Price 2000; Price et al. 2003). Conversely, posterior fusiform to superior temporal gyrus connections are understood as more of a non-semantic route, where low-frequency words and pseudowords would be phonologically decoded prior to engagement of posterior IFG regions (Price 2000; Price et al. 2003). The posterior IFG (i.e., pars opercularis) and the superior temporal gyrus have been repeatedly linked to phonological functions (e.g., IFG: McDermott et al. 2003; Poldrack et al. 1999; STG: Simos et al. 2000, 2002), but their distinct contributions are not understood. Analogously, the inferior temporal gyrus and anterior IFG are both recognized as semantic areas (Devlin et al. 2003; McDermott et al. 2003; Poldrack et al. 1999), but their unique roles in semantic processing have not been characterized.

In the current study, activation in the FUSIp region did not reliably differ between conditions in the earliest latency bin. However, slightly later, our analyses indicated greater activation in ITG-Sp for real words (110–150 ms), along with a significant effect favoring pseudowords in the STG-Sp (95–215 ms). These spatiotemporal dynamics could indicate neural processes in posterior cortices had already discerned the word types, and consequently engaged distinct pathways or mechanisms specialized for different linguistic functions. For words, this translates into early activation of the ITG-Sp, where potentially lexical items can be associated with semantic correlates. Conversely, for pseudowords the preferential pathway transverses STG-Sp initially, where ostensibly stimuli are phonologically decoded before association with semantic correlates is attempted. It is worth noting that FUSIp activation was significantly stronger for pseudowords 185–355 ms into the time course, which could indicate these cortices work in conjunction with the STG-Sp in phonological decoding processes. It may be that FUSIp maintains a memory trace corresponding to graphemic composition of the input stimulus, and transmits such information serially to STG-Sp which then computes appropriate phonemic translations. Such an interpretation of left posterior fusiform function would be consistent with the perceptual interface proposal noted above (Devlin et al. 2006; Price and Devlin 2004; Price and Mechelli 2005). Presumably, the activation decline in FUSIp at ~355 ms indicates grapheme-to-phoneme translation has been completed, which then cues initial attempts at resolving lexical and semantic status of the input stimulus. We favor this interpretation because the offset of FUSIp activation in the pseudoword condition was immediately followed by engagement of IFG cortices (385–415 ms) as well as the ITG-Sp (400–430 ms). Perhaps the STG-Sp transmits a complete phonological representation to posterior IFG, which is known

to contribute to phonological processing (McDermott et al. 2003; Poldrack et al. 1999). With a complete phonological representation, IFG may then interact with ITG-Sp cortices to probe availability of semantic correlates, in order to ultimately resolve lexical status. Lastly, it is important to realize that throughout this time period (until ~430 ms), and the remaining time course, activation in STG-Sp was significantly stronger for pseudowords. Thus, with the exception of early ITG-Sp activation (words > pseudowords), neural resources in all ROIs were more strongly recruited by pseudoword stimuli until ~430 ms post-stimulus onset. This more-or-less global pattern may signify pseudowords place tremendously more burdensome processing demands on the entire linguistic system, a position which is consonant with intuition and also supported by the behavioral data. Moreover, such an overall pattern would be expected if the processing of words but not pseudowords could proceed through a lexicon-like word-based code (i.e., Coltheart et al. 1993, 2001); accordingly, we propose that the relatively limited dynamics amongst word-activated neural regions during this temporal period (i.e., before ~400 ms) supports the notion that lexical processing can utilize word-based codes, as suggested in current dual-mechanism formulations.

However, after ~430 ms, significant effects favoring word stimuli remerged, as more robust activation was detected in two neural regions (i.e., ITG-Sp and IFG). For the ITG-Sp, this reflected the second period of activation during word processing, whereas for the IFG it was the first sign of word-induced activity. Analogous to the pseudoword condition, initial activation of IFG cortices (i.e., 425 ms) was shadowed by engagement of the ITG-Sp region at 435 ms. Although in contrast to pseudowords, we believe the significance of this activity differs in regard to the linguistic processes transpiring. This is the second wave of word-induced activity for ITG-Sp cortex, and presumably the system's current processing status is conceptually different. It is well appreciated that anterior and posterior IFG regions are specialized for distinct linguistic functions; the anterior portion being more involved in semantics and the posterior region playing a larger role in phonological processing (Devlin et al. 2003; McDermott et al. 2003;Poldrack et al. 1999). Perhaps this word-specific activity is more semantic in nature than the analogous pattern culminating in the pseudoword condition some ~30 ms earlier. We contend the linguistic system has likely resolved lexical status prior to this period of activation (i.e., during the earlier period of ITG-Sp activation), and that the current activity reflects selection of the precise semantic correlate of the input stimulus. Furthermore, once a semantic code has been established, the ITG-Sp may go offline leaving the IFG to signal motor cortices to withhold the behavior response (i.e., accepting the candidate as a word meant a no-go response in this task). This contention is supported by ITG-Sp activity (435–465 ms) terminating slightly before that of IFG (425–485 ms). Obviously, the capacity to distinguish anterior from posterior IFG activation would have been beneficial to our argument of fundamentally different processes transpiring in these two regions between the two word classes. However, we decided before the analysis to lump the anterior and posterior IFG into a single ROI, as it was questionable whether anterior and posterior activity could be accurately discerned given the spatial precision of MEG. Thus, we admit the current interpretation is limited due to this uncertainty, but we also argue the different temporal behavior of ITG-Sp and IFG mandates that we consider the possibility of distinct component operations between the different word classes.

By ~485 ms the greater activation to words had dissipated in the IFG, and for the remaining epoch no regions showed significant activity favoring words. This pattern may indicate that linguistic processing had been more-or-less completed, leaving only the planning and execution aspects of the behavioral response some ~100 later. In contrast, for pseudowords activity reemerged in the STG-Sp region at 505–545 ms, and this significantly greater activation coexisted with similar dynamics in the ITG-Sp area (525–555ms). At this latency, the linguistic system may attempt a final pass at resolving lexical status. Essentially, for the system to conclude the input stimulus was a pseudoword, it presumably has to make some form

of comparison, most likely using phonological representations, to all lexical items coded in the memory of the reader. The co-activation of the STG-Sp region, a well-established phonological processing center (Simos et al. 2000, 2002), along with the largely semantic ITG-Sp area may be indicative of such a final pass before the search process is terminated and the lexical candidate is ultimately rejected as a pseudoword. Our behavioral data were consistent with previous lexical-decision experiments showing that pseudowords are rejected significantly slower than words are accepted. We believe the co-activation of these two neural regions, at such a delayed latency, may be indicative of the differential processes necessarily underling these observed behavioral effects. Of course, other interpretations are possible and future research should investigate whether significant effects are present in other neural regions during this same latency range.

Finally, it is important to recognize the limitations of this work including the small sample size, limited number of neural regions investigated, and the unconventional nature of our lexical-decision paradigm, all of which limit the generalizability of the findings. In the current study, we chose to focus on the network of brain regions most commonly accepted as central to language processing (Jobard et al. 2003; Mechelli et al. 2002; Price 2000; Price et al. 2003), so that an in-depth analysis of the dynamics would be more feasible. However, future studies could certainly expand our findings by including more ROI's and a greater number of subjects. Another concern is whether our observations would have differed had a standard lexical-decision paradigm been used. In our task, the block-wise distribution of stimuli was non-conventional; such that, in blocks where pseudowords were targets only words were non-targets, and in blocks where words were targets both pseudowords and consonant strings were non-targets. We also focused all MEG analyses on the non-target stimuli, whereas typically all stimuli are targets and all are analyzed. In developing this experiment, we did not believe such task differences would significantly change the MEG results, and thus we utilized this oddball variant of lexical-decision to garner the benefits of constant behavioral responses across conditions (i.e., no response in either condition) and reduced overall MEG recording time. Although we cannot conclude these task differences did not affect the results, our behavioral data were congruent with other studies that used conventional lexical-decision, suggesting it is at least unlikely that these paradigm modifications significantly impacted our neural data. Lastly, one cannot rule-out the possibility that our activation time series findings merely reflect simple word-frequency differences between words and pseudowords. However, while word-frequency could have mediated the effects observed early in the FUSIp, it is clearly a much less likely explanation for our primary finding of differences in sequential order of activated neural regions between words and pseudowords.

In conclusion, the neural dynamics observed in the current study lend strong support to the neurological model of reading proposed by Price (2000; Price et al. 2003). In this model, words and pseudowords are processed in parallel along two distinct pathways. The semantic pathway preferentially processes real words, and is thought to rely mainly on the left posterior fusiform gyrus, the left inferior temporal gyrus, and the anterior portion of the left inferior frontal gyrus. In contrast, the non-semantic pathway provides crucial contributions to the reading of low-frequency words and pseudowords, and relies more strongly on left posterior fusiform gyrus, left superior temporal gyrus, and the posterior portion of the left inferior frontal gyrus. The current data supports the main tenets of this model, but also extends it by providing temporal structure to the neural correlates. Mainly, processing in both pathways commenced at ~100 ms in the FUSIp region. Activity specific to a certain pathway emerges ~15–20 ms later, and appears in the ITG-Sp for the semantic pathway and in STG-Sp for the non-semantic pathway. Although speculative, the pathway that is preferentially engaged (i.e., possesses the shortest activation latency) is likely contingent on the outcome of initial processes culminating in the FUSIp area. According to the pertinent model, the initial engagement of the preferential pathway is followed by activation of the opposing pathway. This was clearly discernable in

the fixed effects analyses of the current data (see Figure 1), as words first induced ITG-Sp activity which was briefly followed by STG-Sp activation; the opposite sequential order was observed to pseudowords in these two neural regions. Activation along both pathways then engages IFG cortices, with a slightly earlier latency for the non-semantic pathway. Although not spatially discernable in the current data, the temporal structure suggests the IFG node of the semantic pathway (anterior IFG) was engaged significantly later than the IFG node of the non-semantic pathway (posterior IFG). During and following IFG activation, the non-semantic pathway relied heavily on STG-Sp cortices for phonological decoding operations, whereas the semantic pathway utilized ITG-Sp cortices for the majority of necessary linguistic processes. In summary, the current data provide support for a dual-mechanism account of reading (Coltheart et al. 1993, 2001) that utilizes predominantly the neural structures recognized in Price's model (2000; Price et al. 2003). Our most remarkable finding was clearly the reversed order of sequential activations in temporal lobe regions between words and pseudowords. Finally, the current data provide initial evidence for the time course of crucial nodes within each distinct pathway, and for the contention that both pathways are eventually activated by all legal graphemic stimuli (i.e., words and pronounceable pseudowords).

Acknowledgements

Funding for TWW was provided by an Eva O. Miller Endowed Fellowship through the University of Minnesota. ACL and PJP were funded by the Mental Illness and Neuroscience Discovery (MIND) Institute. JEM was funded by NIH/NINDS Grant RO1 NS30914. This work was also supported by the U.S. Department of Veterans Affairs, the American Legion Auxiliary, and the American Legion Brain Sciences Chair.

References

Balota, DA.; Cortese, MJ.; Hutchison, KA.; Neely, JH.; Nelson, D.; Simpson, GB., et al. The English Lexicon Project: A web-based repository of descriptive and behavioral measures for 40,481 English words and nonwords. Washington University; 2002. http://elexicon.wustl.edu/

Binder JR, McKiernan KA, Parsons ME, Westbury CF, Possing ET, Kaufman, JN, et al. Neural correlates of lexical access during visual word recognition. J Cogn Neurosci 2003;15:372–393. [PubMed: 12729490]

Binder JR, Medler DA, Desai R, Conant LL, Liebenthal E. Some neurophysiological constraints on models of word naming. Neuroimage 2005a;27:677–693. [PubMed: 15921937]

Binder JR, Westbury CF, McKiernan KA, Possing ET, Medler DA. Distinct brain systems for processing concrete and abstract concepts. J Cogn Neurosci 2005b;17:905–917. [PubMed: 16021798]

Bowyer SM, Moran JE, Mason KM, Constantinou JE, Smith BJ, Barkley GL, et al. MEG localization of language-specific cortex utilizing MR-FOCUSS. Neurology 2004;62:2247–2255. [PubMed: 15210890]

Cohen L, Dehaene S. Specialization within the ventral stream: The case for the visual word form area. Neuroimage 2004;22:466–476. [PubMed: 15110040]

Coltheart M, Curtis B, Atkins P, Haller M. Models of reading aloud: Dual-route and parallel-distributed-processing approaches. Psychol Rev 1993;100:589–608.

Coltheart M, Rastle K. Serial processing in reading aloud: Evidence for dual-route models of reading. J Exp Psychol Hum Percept Perform 1994;20:1197–1211.

Coltheart M, Rastle K, Perry C, Langdon R, Ziegler J. DRC: A dual-route cascaded model of visual word recognition and reading aloud. Psychol Rev 2001;108:204–256. [PubMed: 11212628]

Cornelissen PL, Tarkiainen A, Helenius P, Salmelin R. Cortical effects of shifting letter position in letter strings of varying length. J Cogn Neurosci 2003;15:731–746. [PubMed: 12965046]

Dale AM, Liu AK, Fischl BR, Buckner RL, Belliveau JW, Lewine JD, Halgren E. Dynamic statistical parametric mapping: Combining fMRI and MEG for high-resolution imaging of cortical activity. Neuron 2000;26:55–67. [PubMed: 10798392]

Dehaene S, Cohen L, Sigman M, Vinckier F. The neural code for written words: A proposal. Trends Cogn Sci 2005;9:335–341. [PubMed: 15951224]

Devlin JT, Jamison HL, Gonnerman LM, Matthews PM. The role of the left fusiform gyrus in reading. J Cogn Neurosci 2006;18:911–922. [PubMed: 16839299]

Devlin JT, Jamison HL, Matthews PM, Gonnerman LM. Morphology and the internal structure of words. Proc Natl Acad Sci USA 2004;101:14984–14988. [PubMed: 15358857]

Devlin JT, Matthews PM, Rushworth MS. Semantic processing in the left inferior prefrontal cortex: A combined functional magnetic resonance imaging and transcranial magnetic stimulation study. J Cogn Neurosci 2003;15:71–84. [PubMed: 12590844]

Dhond RP, Buckner RL, Dale AM, Marinkovic K, Halgren E. Spatiotemporal maps of brain activity underlying word generation and their modification during repetition priming. J Neurosci 2001;21:3564–3571. [PubMed: 11331385]

Dhond RP, Marinkovic K, Dale AM, Witzel T, Halgren E. Spatiotemporal maps of past tense verb inflection. Neuroimage 2003;19:91–100. [PubMed: 12781729]

Duvernoy, HM.; Bourgouin, P.; Cabanis, EA.; Cattin, F.; Guyot, F.; Iba-Zizen, MT., et al., editors. Vol. 2nd ed.. New York: Springer; 1999. The human brain: Surface, blood supply, and three-dimensional sectional anatomy.

Fiebach CJ, Friederici AD, Muller K, von Cramon DY. fMRI evidence for dual routes to the mental lexicon in visual word recognition. J Cogn Neurosci 2002;14:11–23. [PubMed: 11798383]

Frith U, Wimmer H, Landerl K. Differences in phonological recoding in German- and English-speaking children. Scientific Study of Reading 1998;2:31–54.

Hämäläinen MS, Sarvas J. Realistic conductivity geometry model of the human head for interpretations of neuromagnetic data. IEEE Trans Biomed Eng 1989;36:165–171. [PubMed: 2917762]

Ischebeck A, Indefrey P, Usui N, Nose I, Hellwig F, Taira M. Reading in a regular orthography: An fMRI study investigating the role of visual familiarity. J Cogn Neurosci 2004;16:727–741. [PubMed: 15200701]

Jerbi K, Baillet S, Mosher JC, Nolte G, Garnero L, Leahy RM. Localization of realistic cortical activity in MEG using current multipoles. Neuroimage 2004;22:779–793. [PubMed: 15193607]

Jobard G, Crivello F, Tzourio-Mazoyer N. Evaluation of the dual route theory of reading: A metanalysis of 35 neuroimaging studies. Neuroimage 2003;20:693–712. [PubMed: 14568445]

Keller TA, Carpenter PA, Just MA. The neural basis of sentence comprehension: A fMRI examination of syntactic and lexical processing. Cereb Cortex 2001;11:223–237. [PubMed: 11230094]

Kucera, H.; Francis, WN. Providence: Brown University Press; 1967. Computational analysis of present-day American English.

Kronbichler M, Hutzler F, Wimmer H, Mair A, Staffen W, Ladurner G. The visual word form area and the frequency with which words are encountered: Evidence from a parametric fMRI study. Neuroimage 2004;21:946–953. [PubMed: 15006661]

Kuo WJ, Yeh TC, Lee CY, Wu YT, Chou CC, Ho LT, et al. Frequency effects of Chinese character processing in the brain: An event related fMRI study. Neuroimage 2003;18:720–730. [PubMed: 12667849]

Landerl K, Wimmer H, Frith U. The impact of orthographic consistency on dyslexia: A German-English comparison. Cognition 1997;63:315–334. [PubMed: 9265873]

Leahy RM, Mosher JC, Spencer ME, Huang MX, Lewine JD. A study of dipole localization accuracy for MEG and EEG using a human skull phantom. Clin Neurophysiol 1998;107:159–173.

Leuthold AC. Subtraction of heart artifact from MEG data: The matched filter revisited. Soc Neurosci Abstracts 2003;15:863.

Marinkovic K, Dhond RP, Dale AM, Glessner M, Carr V, Halgren E. Spatiotemporal dynamics of modality-specific and supramodal word processing. Neuron 2003;38:487–497. [PubMed: 12741994]

McDermott KB, Peterson SE, Watson JM, Ojemann JG. A procedure for identifying regions preferentially activated by attention to semantic and phonological relations using functional magnetic resonance imaging. Neuropsychologia 2003;41:293–303. [PubMed: 12457755]

Mechelli A, Gorno-Tempini ML, Price CJ. Neuroimaging studies of word and pseudoword reading: Consistencies, inconsistencies, and limitations. J Cogn Neurosci 2003;15:260–271. [PubMed: 12676063]

Mechelli A, Penny WD, Price CJ, Gitelman DR, Friston KJ. Effective connectivity and intersubject variability: Using a multisubject network to test differences and commonalities. NeuroImage 2002;17:1459–1469. [PubMed: 12414285]

Moran, JE.; Tepley, N. MEG Tools: Imaging and visualization software. http://www.megimaging.com.

Moran JE, Bowyer SM, Tepley N. Multi-resolution FOCUSS source imaging of MEG data. Biomed Tech (Berl) 2001;46:112–114.

Moran JE, Bowyer SM, Tepley N. Multi-resolution FOCUSS: A source imaging technique applied to MEG data. Brain Topogr 2005;18:1–17. [PubMed: 16193262]

Oldfield RC. The assessment and analysis of handedness: The Edinburgh inventory. Neuropsychologia 1971;9:97–113. [PubMed: 5146491]

Pammer K, Hansen PC, Kringelbach ML, Holliday I, Barnes G, Hillebrand A, et al. Visual word recognition: The first half second. Neuroimage 2004;22:1819–1825. [PubMed: 15275938]

Paulesu E, McCrory E, Fazio F, Menoncello L, Brunswick N, Cappa SF, et al. A cultural effect on brain function. Nat Neurosci 2000;3:91–96. [PubMed: 10607401]

Petersen SE, Fox PT, Posner MI, Mintun M, Raichle ME. Positron emission tomographic studies of the cortical anatomy of single-word processing. Nature 1988;331:585–589. [PubMed: 3277066]

Plaut DC, McClelland JL, Seidenberg MS, Patterson KE. Understanding normal and impaired word reading: Computational principles in quasi-regular domains. Psychol Rev 1996;103:56–115. [PubMed: 8650300]

Poldrack RA, Wagner AD, Prull MW, Desmond JE, Glover GH, Gabrieli JDE. Functional specialization for semantic and phonological processing in the left inferior prefrontal cortex. NeuroImage 1999;10:15–35. [PubMed: 10385578]

Price CJ. The anatomy of language: Contributions from functional neuroimaging. J Anat 2000;197:335–359. [PubMed: 11117622]

Price CJ, Devlin JT. The pro and cons of labeling a left occipitotemporal region: “The visual word form area.”. Neuroimage 2004;22:477–479. [PubMed: 15110041]

Price CJ, Gorno-Tempini ML, Graham KS, Biggio N, Mechelli A, Patterson K, Noppeney U. Normal and pathological reading: Converging data from lesion and imaging studies. Neuroimage 2003;20:S30–S41. [PubMed: 14597294]

Price CJ, Mechelli A. Reading and reading disturbance. Curr Opin Neurobiol 2005;15:231–238. [PubMed: 15831408]

Rissman J, Eliassen JC, Blumstein SE. An event-related fMRI investigation of implicit semantic priming. J Cogn Neurosci 2003;15:1160–1175. [PubMed: 14709234]

Seidenberg MS, McClelland JL. Distributed, developmental model of word recognition and naming. Psychol Rev 1989;96:523–568. [PubMed: 2798649]

Simos PG, Breier JI, Wheless JW, Maggio WM, Fletcher JM, Castillo EM, Papanicolaou AC. Brain mechanisms for reading: The role of the superior temporal gyrus in word and pseudoword naming. Neuroreport 2000;11:2443–2447. [PubMed: 10943701]

Simos PG, Breier JI, Fletcher JM, Foorman BR, Castillo EM, Papanicolaou AC. Brain mechanisms for reading words and pseudowords: An integrated approach. Cereb Cortex 2002;12:297–305. [PubMed: 11839603]

Wilson TW, Leuthold AC, Lewis SM, Georgopoulos AP, Pardo PJ. The time and space of lexicality: A neuromagnetic view. Exp Brain Res 2005a;162:1–13. [PubMed: 15517213]

Wilson TW, Leuthold AC, Lewis SM, Georgopoulos AP, Pardo PJ. Cognitive dimensions of orthographic stimuli affect occipitotemporal dynamics. Exp Brain Res 2005b;167:141–147. [PubMed: 16096785]

Xu B, Grafman J, Gaillard WD, Ishii K, Vega-Bermudez F, Pietrini P, et al. Conjoint and extended neural networks for the computation of speech codes: The neural basis of selective impairment in reading words and pseudowords. Cereb Cortex 2001;11:267–277. [PubMed: 11230098]

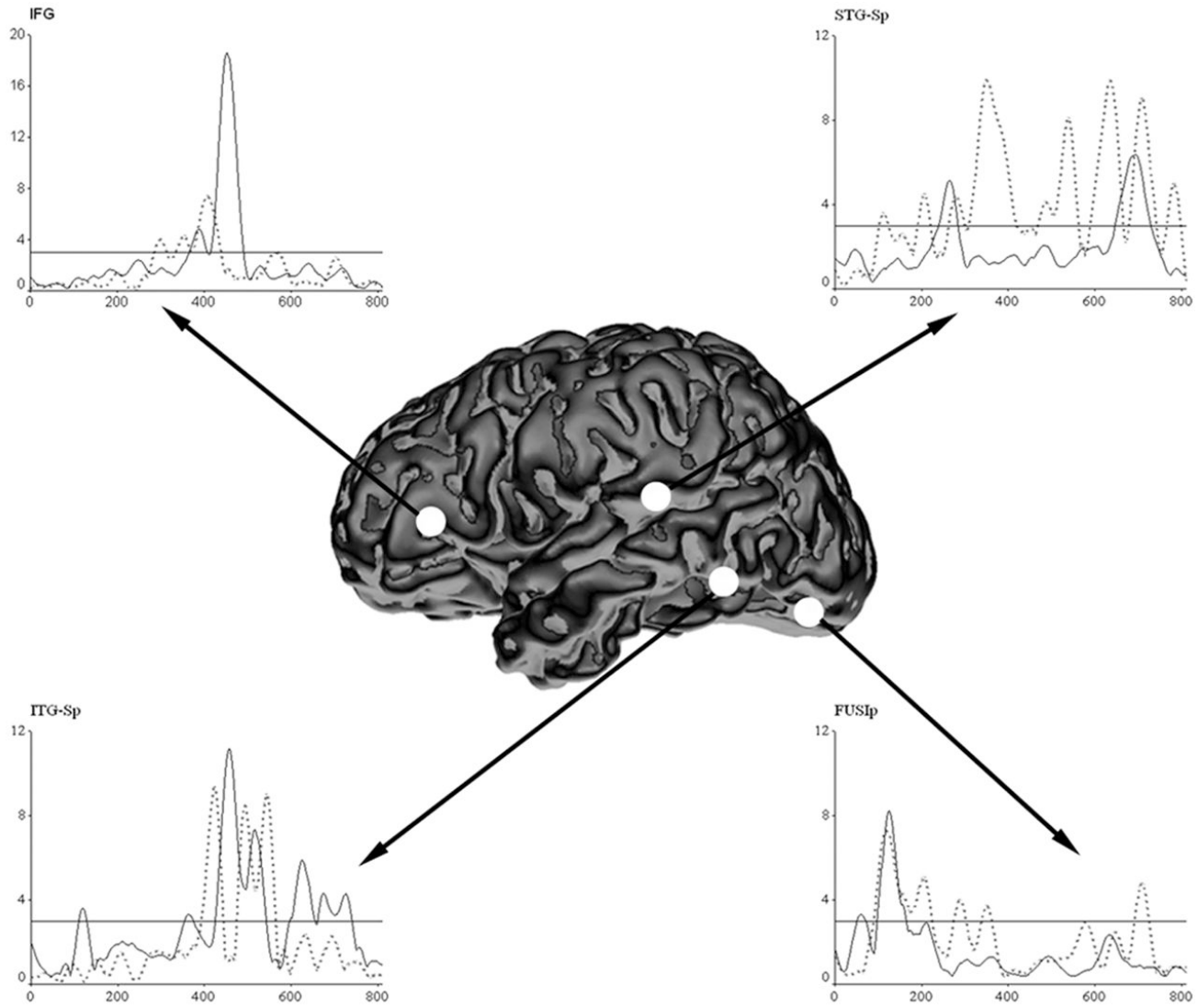

Figure 1.

Grand average waveforms for each condition in the four ROIs. The average time course of the noise-normalized current-density estimates for each ROI in the word (solid black line) and pseudoword (dotted gray line) conditions are displayed above. The white circles on the standardized 3D rendition indicate the cortical area corresponding to each activation time course plot. Time is displayed on the abscissa in ms units, whereas the activity estimates are displayed on the ordinate in SD units. In each plot, a reference line marks the $p < 0.001$ activation threshold for the given ROI. As shown, the sequential order of activated temporal lobe regions was reversed for the two word classes, as words initially activated ITG-Sp and then the STG-Sp region; the opposite was observed to pseudowords. Note that the scale of the ordinate axis differs between ROIs.

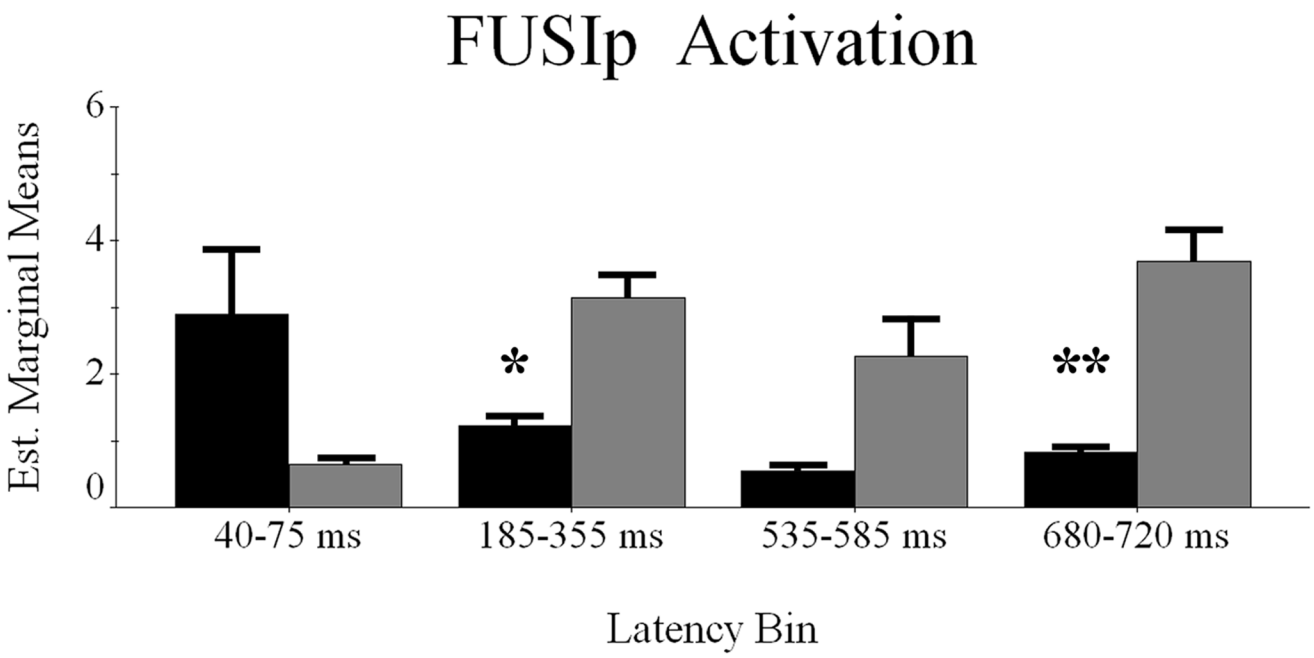

Figure 2.

Latency periods of maximal contrast between word classes in the FUSIp region. The four latency bins of interest are graphed separately on the abscissa with words represented in black and pseudowords in gray. The estimated marginal means of the activity amplitude estimates are displayed on the ordinate. Error bars depict one standard error of the mean. Significant differences between words and pseudowords within a latency bin are denoted with asterisk(s). * = $p < 0.05$; ** = $p < 0.01$

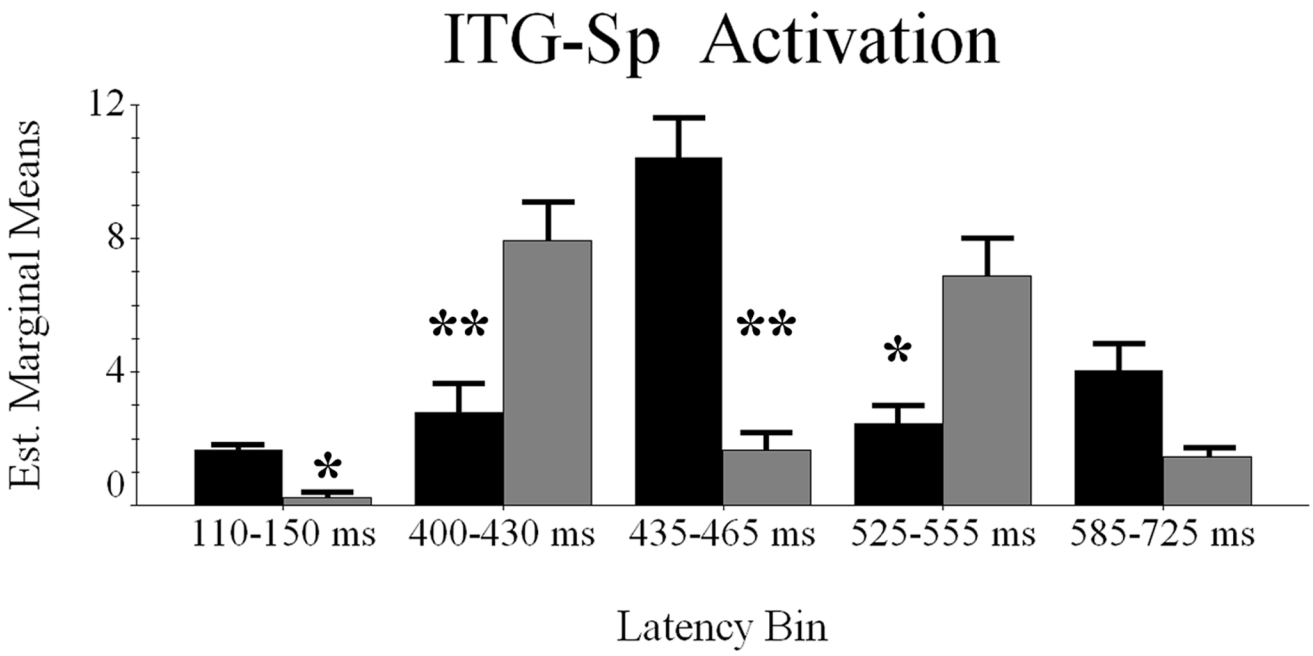

Figure 3.
Latency periods of maximal contrast between word classes in the ITG-Sp area. The abscissa and ordinate are the same as Figure 2, and words are again represented in black with pseudowords in gray. Error bars depict one standard error of the mean, and asterisk(s) denote significant differences. * = $p < 0.05$; ** = $p < 0.01$

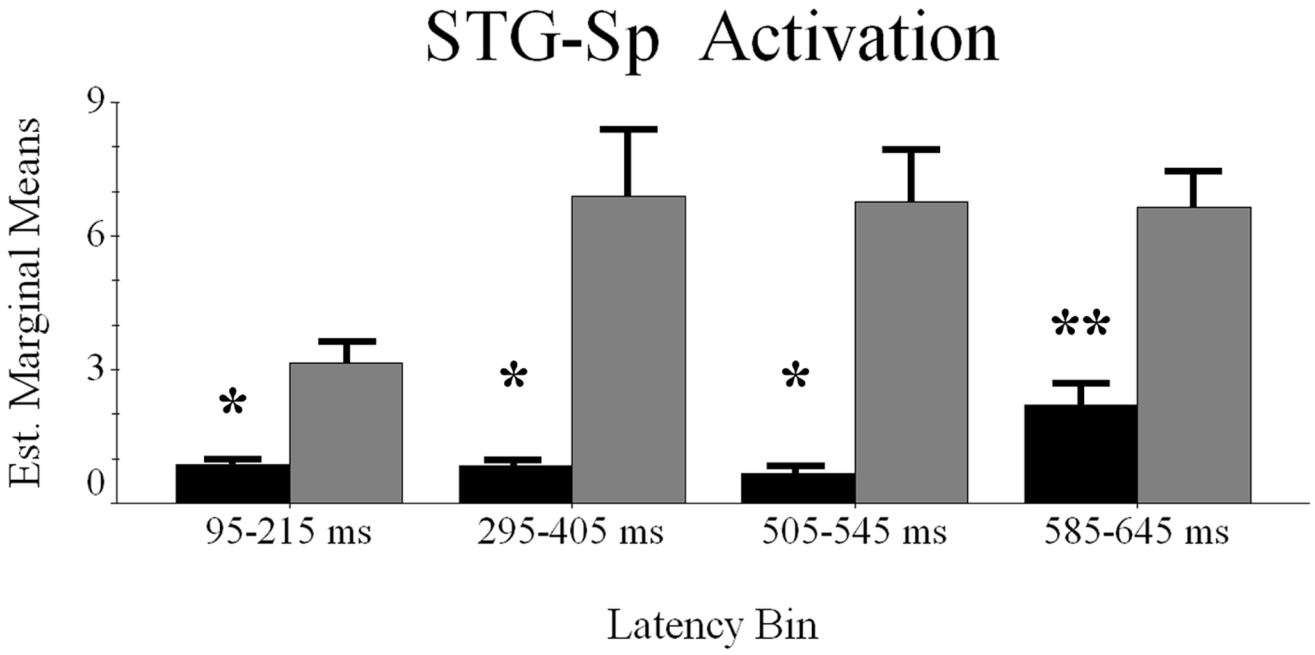

Figure 4.

Latency periods of maximal contrast between word classes in the STG-Sp region. Words are shown in black and pseudowords in gray; the abscissa and ordinate are also the same as in Figure 2–Figure 3. Error bars depict one standard error of the mean. Significant differences between the conditions within each time bin are denoted with asterisk(s). * = $p < 0.05$; ** = $p < 0.01$

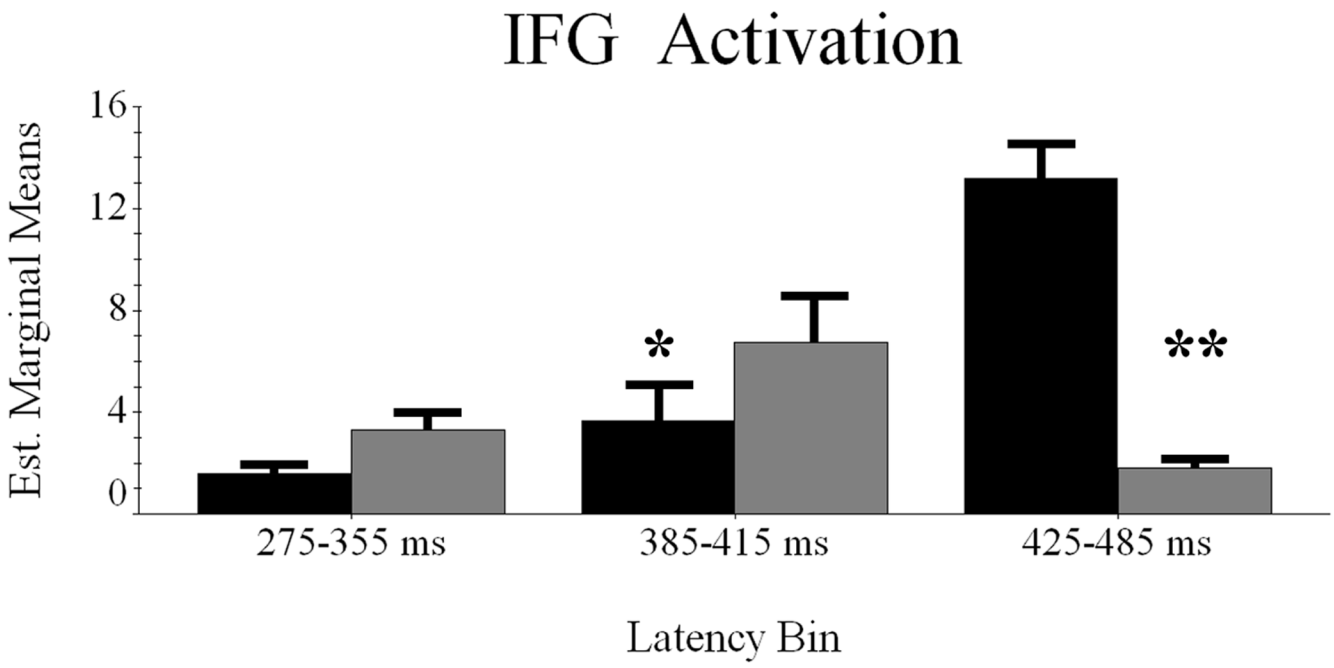

Figure 5.

Latency periods of maximal contrast between word classes in IFG cortices. The abscissa and ordinate are the same as Figure 2 – Figure 4, with words represented in black with pseudowords in gray. The error bars depict one standard error of the mean, and asterisk(s) denote significant differences between words and pseudowords within each latency period. * = $p < 0.05$; ** = $p < 0.01$